Profilin connects actin assembly with microtubule dynamics

Michaela Nejedla[a], Sara Sadi[a], Vadym Sulimenko[b], Francisca Nunes de Almeida[c,†], Hans Blom[d], Pavel Draber[b], Pontus Aspenström[c], and Roger Karlsson[a,*]

[a]Department of Molecular Biosciences, Wenner-Gren Institute, Stockholm University, SE-106 91 Stockholm, Sweden; [b]Institute of Molecular Genetics, ASCR, 142 20 Prague 4, Czech Republic; [c]Department of Microbiology, Tumor and Cell Biology, Karolinska Institutet, SE-171 77 Stockholm, Sweden; [d]Science for Life Laboratory, SE-171 21 Solna, Sweden

ABSTRACT **Profilin controls actin nucleation and assembly processes in eukaryotic cells. Actin nucleation and elongation promoting factors (NEPFs) such as Ena/VASP, formins, and WASP-family proteins recruit profilin:actin for filament formation. Some of these are found to be microtubule associated, making actin polymerization from microtubule-associated platforms possible. Microtubules are implicated in focal adhesion turnover, cell polarity establishment, and migration, illustrating the coupling between actin and microtubule systems. Here we demonstrate that profilin is functionally linked to microtubules with formins and point to formins as major mediators of this association. To reach this conclusion, we combined different fluorescence microscopy techniques, including superresolution microscopy, with siRNA modulation of profilin expression and drug treatments to interfere with actin dynamics. Our studies show that profilin dynamically associates with microtubules and this fraction of profilin contributes to balance actin assembly during homeostatic cell growth and affects microtubule dynamics. Hence profilin functions as a regulator of microtubule (+)-end turnover in addition to being an actin control element.**

Monitoring Editor
Laurent Blanchoin
CEA Grenoble

Received: Nov 23, 2015
Revised: Jun 8, 2016
Accepted: Jun 9, 2016

INTRODUCTION

Actin polymerization—the directional growth of actin filaments as a consequence of ordered addition of new actin subunits at the favored (+)-end of the filament—is a fundamental and tightly regulated process required for numerous cellular phenomena. The structural and biochemical asymmetry of the filaments form the basis for the directional force generation. This is kinetically maintained by hydrolysis of ATP on the incoming actin subunit soon after its association at the filament (+)-end (Melki *et al.*, 1996; Nyman *et al.*, 2002b) and is under control of an array of actin-binding proteins by which different (+)-end–tracking proteins (commonly referred to as nucleation and elongation–promoting factors [NEPFs]), such as enabled/vasodilator-stimulated phosphoprotein (Ena/VASP) and formins, govern processivity and elongation speed (Bugyi and Carlier, 2010; Grantham *et al.*, 2012).

Although the importance of actin for cell migration and particularly for the advancement of the cell edge is well established (e.g., Pollard and Borisy, 2003; Le Clainche and Carlier, 2008), it has long been known that directional cell movement typically also requires an intact microtubule system (Vasiliev *et al.*, 1970; Tint *et al.*, 1991; Kaverina *et al.*, 1998). It is now clear that the two force-generating systems operate closely together to coordinate cell architectonics and behavior (Small *et al.*, 2002; Rodriguez *et al.*, 2003; Chesarone *et al.*, 2010; Rottner *et al.*, 2010). Many details of the actin–microtubule interplay remain to be resolved, however, not least with respect

This article was published online ahead of print in MBoC in Press (http://www.molbiolcell.org/cgi/doi/10.1091/mbc.E15-11-0799) on June 15, 2016.

†Present address: MRC Laboratory for Molecular Cell Biology, London WC1E 6BT, United Kingdom.

*Address correspondence to: Roger Karlsson (roger.karlsson@su.se).

Abbreviations used: APC, adenomatous polyposis coli; Arp2/3, actin-related proteins 2/3; CTN, citrine; CytD, cytochalasin D; Dia 1, Diaphanous 1; EB, end binding; Ena/VASP, enabled/vasodilator-stimulated phosphoprotein; FH, formin homology; GFP, green fluorescent protein; GST, glutathione *S*-transferase; Jasp, jasplakinolide; MAP, microtubule-associated protein; NEPF, nucleation and elongation–promoting factor; Pfn, profilin; PLA, proximity ligation assay; SMIFH2, small-molecule inhibitor of formin homology 2; STED, stimulated emission depletion; +TIP, microtubule plus end–tracking protein; TIRF, total internal reflection fluorescence; WASP, Wiskott–Aldrich syndrome protein; WHAMM, WASP homologue associated with actin, membranes, and microtubules.

to the possible coordination of microtubule-dependent cargo transport and actin polymerization (e.g., Martin *et al.*, 2005; Shen *et al.*, 2012). Here we address this issue with a focus on profilin and its role as a central control component of actin dynamics and assembly.

The profilin:actin complex is the most important species of polymerization-competent nonfilamentous actin in most cells (Kaiser *et al.*, 1999; Lindberg *et al.*, 2008; Pernier *et al.*, 2016), where it operates by providing ATP-bound actin to NEPFs in support of the propulsion of various intracellular structures, as well as in the formation and elongation of surface protrusions such as lamellipodia and filopodia (Suetsugu *et al.*, 1998; Hajkova *et al.*, 2000; Grenklo *et al.*, 2003; Li *et al.*, 2008). Actin dissociating from filament (–)ends is sequestered by cofilin, and, by not fully understood processes involving Srv2/cyclase-associated protein and coronin (e.g., Bertling *et al.*, 2007; Chaudhry *et al.*, 2010; Mikati *et al.*, 2015), the actin monomers reassociate with profilin and are recharged with ATP and ready for a new round of NEPF-controlled polymerization. Recent observations demonstrate that profilin has a key role in balancing actin availability for different NEPF-driven actin assembly processes, particularly by favoring formin and VASP-driven polymerization over actin-related protein 2 and 3 (Arp2/3)–dependent filament formation (Henty-Ridilla and Goode, 2015; Rotty *et al.*, 2015; Suarez *et al.*, 2015). The role of profilin as a central coordinator of actin filament barbed-end growth is also emphasized by observations made in vitro (Pernier *et al.*, 2016).

As with actin, the microtubule system is subject to extensive dynamics also in interphase cells, in which microtubule (+)-ends extend through the cytoplasm toward the cell edge. Not only are the microtubule (+)-ends engaged in association/dissociation of α/β-tubulin heterodimers, but they also harbor a dynamic complex of associated proteins, the so-called microtubule plus end–tracking proteins (+TIPs; Akhmanova and Steinmetz, 2008; Gupta *et al.*, 2014), which are involved in controlling microtubule (+)-end dynamics and function. Of these, the adenomatous polyposis coli (APC) and end-binding (EB) proteins have been shown to interact with Diaphanous (Dia)-related formins, a major actin NEPF family (Wen *et al.*, 2004; Okada *et al.*, 2010). Hence the +TIP-complex forms a molecular link to actin organization. Other components to participate in organizing actin dynamics in association with microtubules are WASP homologue associated with actin, membranes, and microtubules (WHAMM) and Wasp and Scar homologue, which are microtubule-binding members of the Wiskott–Aldrich syndrome protein (WASP) superfamily of proteins and operate along with Arp2/3 to nucleate actin polymerization (Campellone *et al.*, 2008; Gad *et al.*, 2012; Shen *et al.*, 2012; Blom *et al.*, 2015). Moreover, formins have also been observed to associate along microtubule polymers and influence their stability (Bartolini *et al.*, 2008, 2012; Thurston *et al.*, 2012).

We previously noted a partial colocalization of profilin with microtubules in human fibroblasts (Grenklo *et al.*, 2004) and later reported that the proper distribution of profilin mRNA depends on microtubules (Johnsson and Karlsson, 2010). Profilin (unless otherwise stated, profilin refers to the ubiquitous profilin isoform I) has been located in a broad range of cultured cells by the use of different profilin antibodies and fluorescence microscopy (e.g., Mayboroda *et al.*, 1997; Grenklo *et al.*, 2004; Li *et al.*, 2008). Typically, the protein takes a general distribution, sometimes in a fenestrated pattern of fine dots, and accumulates toward the perinuclear region, as well as in a thin "band" along the leading cell edge. In the present study, we show that profilin influences the control of microtubule dynamics, further adding to the conjecture of a close actin–microtubule interrelationship and underscoring profilin as a unique regulator of force generation and cellular behavior in eukaryotes.

RESULTS

Profilin codistributes with microtubules

Studies of the specific subcellular localization of profilin are complicated by an apparent overall fluorescence, reflecting its abundance and juxtamembrane accumulation separately or in complex with actin (profilin:actin). This prevents the visualization of specific but less common cytoplasmic niches other than the plasma membrane where the protein may be located. To circumvent the problem with the disguising diffuse fluorescence, we introduced a brief detergent treatment under microtubule-stabilizing conditions before the cells were fixed (Figure 1A). With the overall diffuse fluorescence dramatically reduced, partial labeling of the microtubule system was clearly revealed. Independent use of the proximity ligation assay (PLA; Soderberg *et al.*, 2006) without detergent pretreatment and of different subsets of profilin:actin antibodies in combination with antibodies to tubulin and kinesin further supported the localization of profilin at or in close proximity with microtubules (Figure 1, B and C, and Supplemental Figure S1). This was also observed by superresolution stimulated emission depletion (STED) microscopy, by which the profilin staining was found to decorate a majority of the microtubules in a fine-dotted pattern (Figure 1D).

Prompted by these results, we decided to analyze microtubule–profilin association further with an approach in which cells, before lysis, were incubated with the microtubule- stabilizing and -destabilizing drugs Taxol and nocodazole, respectively. The resulting extracts were then centrifuged to partition microtubules with their associated components from the rest of the material. Western blotting of the samples showed cosedimentation of profilin with the microtubules after Taxol treatment (Figure 2A). In contrast, the corresponding samples of non–drug-treated cells or cells exposed to nocodazole displayed dramatically less profilin in the pelleted fraction, essentially confirming the immunohistochemical results on a profilin–microtubule interaction. Densitometry of the Western blot result demonstrated an approximately fourfold-increased amount of profilin in the pelleted material after Taxol treatment compared with untreated cells (Figure 2B). On the basis of the foregoing results, we concluded that a fraction of total cellular profilin is associated with the microtubule system. We then decided to overexpress a profilin–citrine fusion construct in order to increase the yield in coimmunoprecipitation experiments in which we used antibodies to green fluorescent protein (GFP)/citrine. Under such conditions, tubulin was detected as a binding partner to the fusion protein, and this result was corroborated by total internal reflection fluorescence (TIRF) microscopy of cells, by which the profilin–citrine fusion was found to codistribute with the microtubules (Figure 2, C–E).

Tubulin has been captured from a brain tissue extract on a profilin column (Witke *et al.*, 1998), but no compelling evidence has been presented for a direct interaction between the two proteins. This issue was addressed here by in vitro experiments in which profilin was combined with either preformed microtubules or tubulin before the onset of polymerization (Supplemental Figure S2). Because no interaction or influence of profilin was observed in these assays, we conclude that the foregoing observations reflect an indirect recruitment of profilin to the microtubule system.

Modulating actin dynamics shifts profilin to and from the microtubule compartment

We then turned to investigate whether the association of profilin with actin was related to its codistribution with the microtubules.

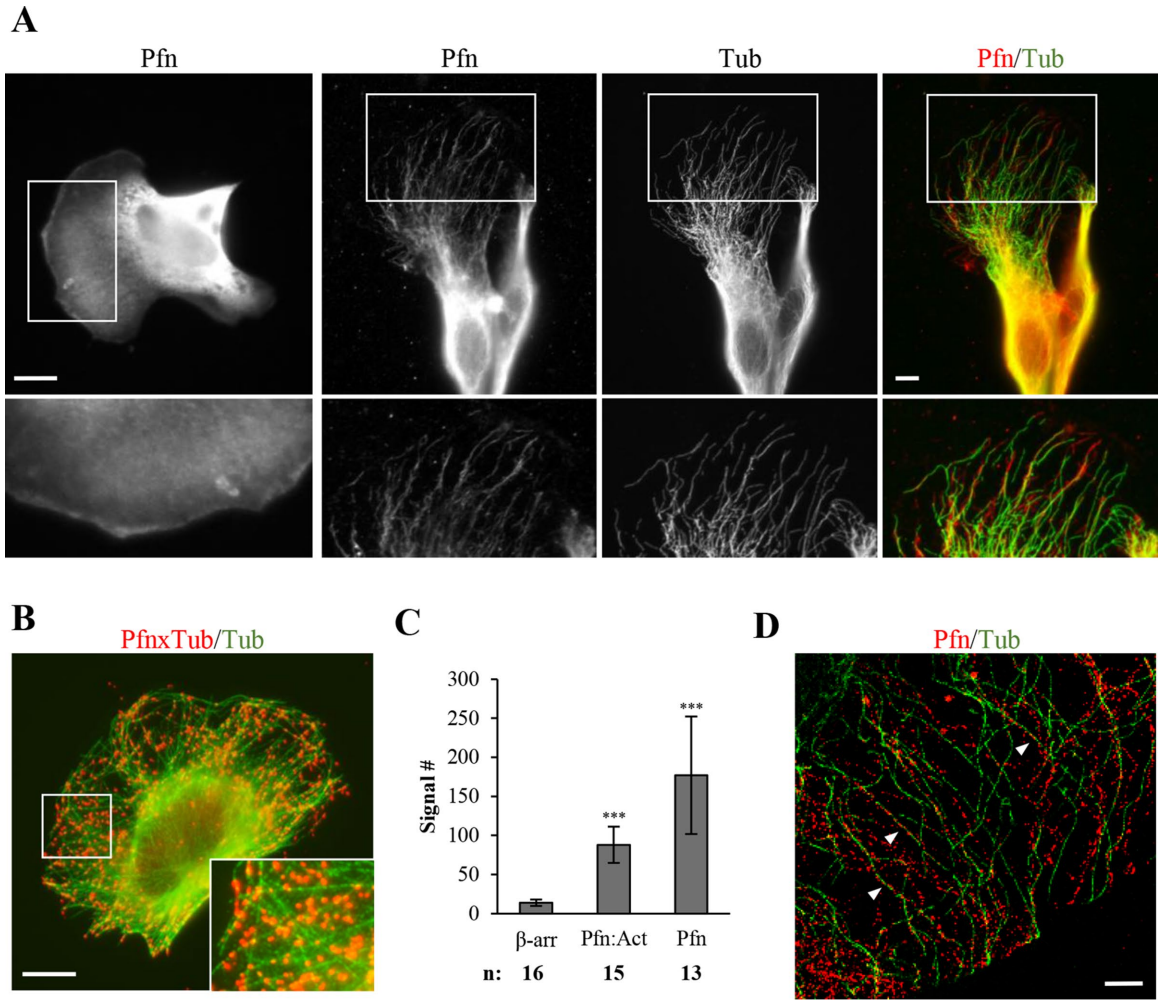

FIGURE 1: Profilin codistributes with microtubules. (A) B16 cells were stained with profilin (Pfn) or α-tubulin (Tub) antibodies. The general distribution of profilin as it is seen after fixation and detergent treatment is displayed at the far left. In striking contrast, as illustrated next, the profilin codistribution with microtubules becomes visible after pretreatment with 0.1% Triton X-100 before fixation. Marked areas are shown below at higher magnification. (B) PLA with a combination of profilin and tubulin antibodies. The microtubule system was visualized using a tubulin antibody from a different species than for the PLA assay (*Materials and Methods*). (C) Signal density from three PLA experiments in which the tubulin antibodies were combined with antibodies as indicated: β-arrestin (β-arr; included as a control) and two different profilin/profilin:actin antibodies (Pfn/Pfn:Act, generated against cross-linked profilin:actin and affinity purified against profilin and actin, respectively). Signal # denotes total number of PLA-marks in four regions of a total area of 26.4 μm^2/cell. (D) The presence of profilin in a dotted pattern along microtubules (arrowheads) as seen by superresolution STED microscopy. Cells were treated with DMSO as in Figure 3. Manders colocalization coefficient (Dunn *et al.*, 2011) was determined to be 0.79 (27 cells; three independent experiments), that is, 79% of the microtubules within the region were associated with profilin at least once along their lengths; see also Figure 3 and Supplemental Figure S5. Student's *t* test, ***$p \leq 0.001$; n = number of cells (three independent experiments, approximately equal number of cells in each experiment); error bars indicate SEM. Scale bars, 10 μm (A), 25 μm (B), 2.5 μm (C).

Exposing cells to cytochalasin D (CytD), which blocks filament barbed-end elongation, or jasplakinolide (Jasp), which increases actin polymerization by stabilizing the filaments, led to an increase of profilin along microtubules (Figure 3, A and B). The shifted localization of profilin to the microtubule-based compartment was readily observed by standard fluorescence microscopy using demembranation before fixation as described earlier (Figure 1). That the two drugs did not cause a variable result despite their different interference with actin polymerization is likely to reflect the fact that we locate both profilin and profilin:actin by microscopy analysis. Interfering with actin polymerization by CytD will increase the concentration of monomeric actin and therefore augment formation of profilin:actin, whereas the filament-stabilizing effect of Jasp may have the opposite effect on the pool of nonfilamentous actin and thereby increase the concentration of "free" profilin. This interpretation explains why we observed an increased amount of profilin associated with microtubules after both drug treatments. To test whether a massive up-regulation of lamellipodia formation with major actin polymerization and engagement of profilin would alter profilin's codistribution with microtubules, we exposed the cells to AlF_4. This is known to dramatically increase actin polymerization due to extensive activation of Rho GTPases and thereby cause formation of

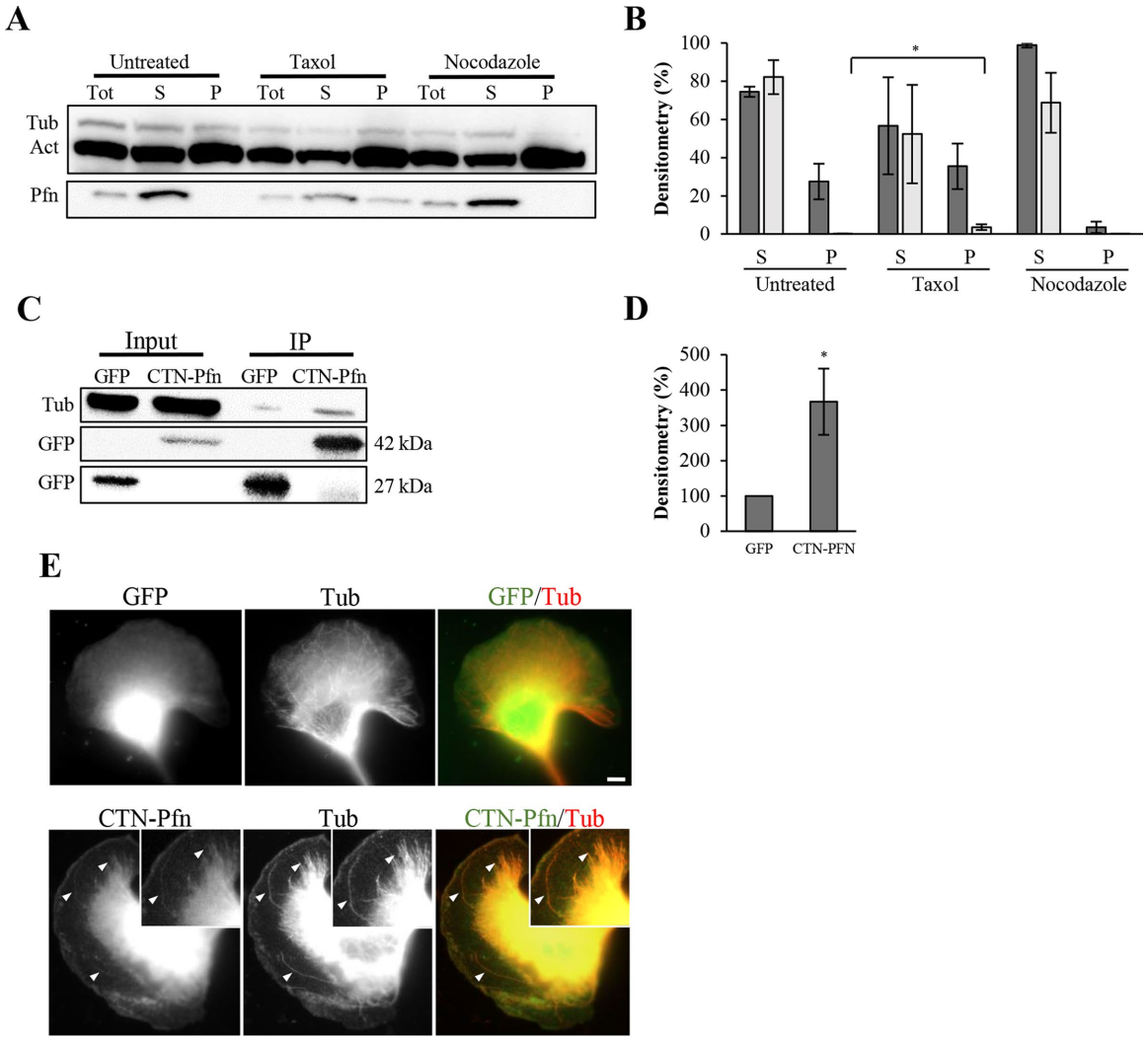

FIGURE 2: Profilin copartitions with microtubules and coimmunoprecipitates with tubulin. (A) Cells were treated with Taxol or nocodazole before lysis, followed by centrifugation to analyze for microtubule copartitioning of profilin by Western blot. P, pellet; S supernatant; Tot, total extracts. Protein bands are identified on the left: tubulin (Tub), actin (Act), and profilin (Pfn). (B) Densitometry of the tubulin (dark gray) and profilin (light gray) bands after analysis as in A and normalized against actin; three independent experiments. Pelleted profilin can be observed only in extracts of Taxol-treated cells. (C) Coimmunoprecipitation analysis after expression of a citrine-profilin fusion (CTN-Pfn), cell lysis, and incubation of the extracts (as indicated on top) with beads conjugated with GFP antibodies followed by Western blot of the captured material with antibodies against tubulin and GFP (left). (D) Densitometry of the GFP/citrine-profilin bands after coimmunoprecipitation as in C, top. GFP indicates the control cell extract. Student's *t* test, $*p \leq 0.05$. Three independent experiments. Values were normalized against input, and error bars indicate SEM. (E) TIRF microscopy was used to visualize codistribution of CTN-Pfn with microtubules after fixation and staining with tubulin antibodies. Arrowheads (bottom) point to profilin localizing along microtubules; inset, higher magnification. Scale bars, 5 μm.

broad lamellipodia at advancing cell edges (Hahne *et al.*, 2001). Accordingly, the AlF_4-treated cells typically displayed up-regulated motility under these conditions, and this was coupled to a dramatic decrease of profilin codistribution with microtubules (Figure 4). Hence we conclude that the actin polymerization status balances the location of profilin to the microtubule system, extending the emerging view of profilin as a pivot for actin monomers between different assembly organizations in the cell (Henty-Ridilla and Goode, 2015).

Possible profilin–microtubule linker molecules

There are several actin assembly components that may be involved in connecting profilin to the microtubule system. The WASP-related protein WHAMM is one of those. It is known to bind microtubules and operates as an actin nucleation–promoting factor due to a W domain, which is preceded by a proline-rich sequence (Campellone *et al.*, 2008; Rottner *et al.*, 2010; Supplemental Figure S3, A and B). Formins represent another family of proteins in this category of microtubule-binding components that carry a proline-rich sequence (Rottner *et al.*, 2010; Thurston *et al.*, 2012). Given the well-documented polyproline-binding activity of profilin, we hypothesized that either or both of these actin NEPFs were involved in linking profilin and/or profilin:actin to the microtubules. Although the interaction between profilin and formins is well established, it was necessary to test whether profilin expresses a similar interaction property for WHAMM. To that end, we expressed a glutathione *S*-transferase

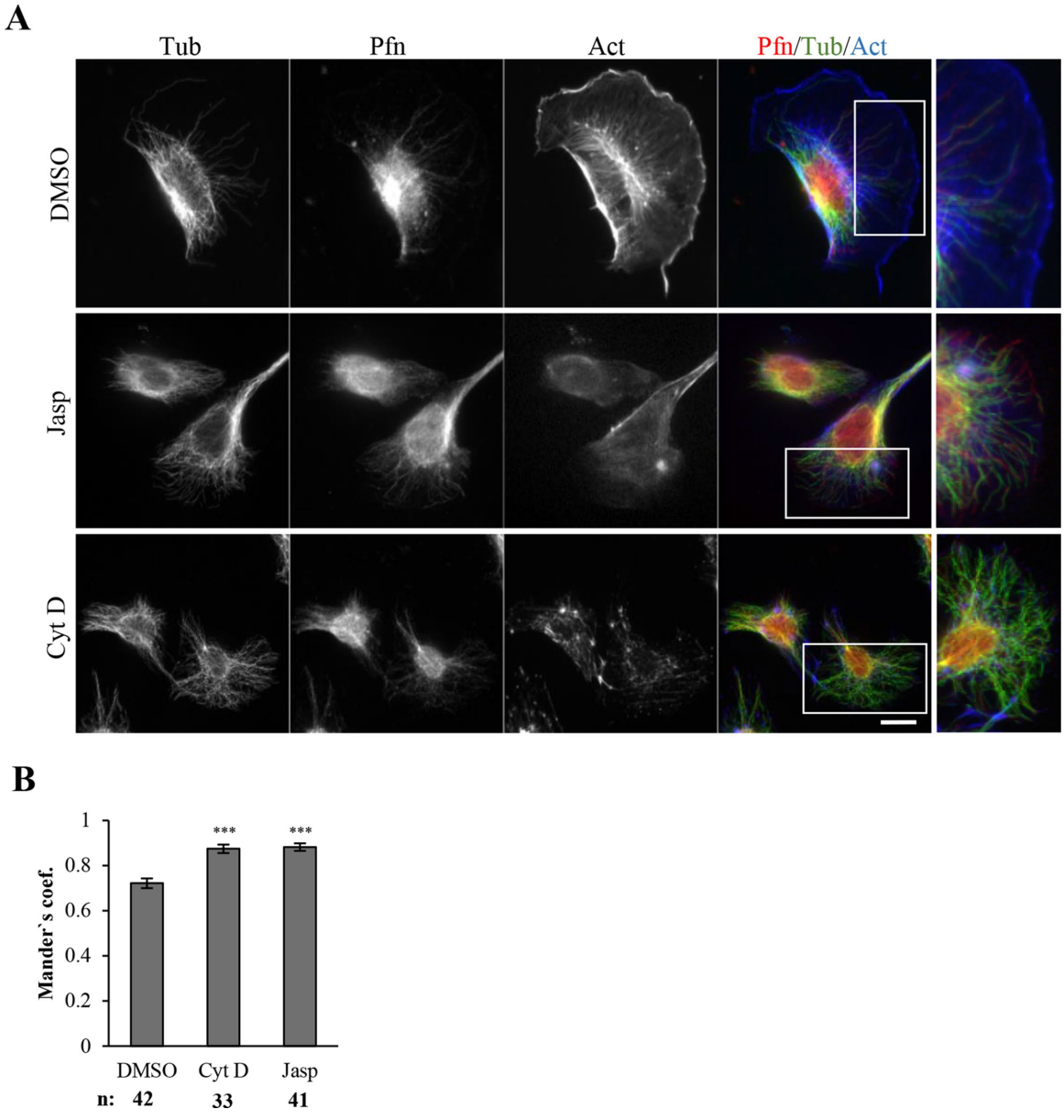

FIGURE 3: Profilin–microtubule association is influenced by actin polymerization status. (A) B16 cells were exposed to 0.1% DMSO (vehicle), 0.5 μM CytD, and 50 nM Jasp for 30 min, followed by detergent pretreatment and fixation as in Figure 1A. The distribution of profilin (red) and tubulin (green) is displayed along with filamentous actin, using SiR-actin (blue); marked areas (merge only) are shown at higher magnification to the right. (B) Extent of profilin–microtubule colocalization after drug treatment as in A, using Manders colocalization coefficient (Dunn *et al.*, 2011) as in Figure 1 and as further explained in Supplemental Figure S5. Two independent experiments; statistics as in Figure 1. Scale bar, 10 μm.

(GST) fusion of a truncated WHAMM construct (WHAMM/C; residues 559–809) that contains a polyproline sequence in *Escherichia coli* and used it for pull-down experiments from cell lysates followed by Western blot analysis with antibodies to profilin. The result showed that under these conditions, profilin indeed is an interaction partner of WHAMM (Supplemental Figure S3C).

Like other WASP-subfamily proteins, WHAMM requires the Arp2/3 complex to function as an actin nucleator. Given that this group of actin NEPFs constitutes a central mechanism for balancing profilin-controlled actin assembly (Rotty *et al.*, 2015; Suarez *et al.*, 2015), we analyzed this activity with respect to the profilin–microtubule interaction using the Arp2/3 inhibitor CK-666 and small interfering RNA (siRNA) down-regulation of WHAMM expression, respectively. However, none of these approaches resulted in an altered distribution of profilin to microtubules, as observed after fluorescence microscopy of pre-demembranated B16 cells (Supplemental Figure S3D), suggesting that WHAMM/Arp2/3 is not a major component in the recruitment of profilin/profilin:actin to the microtubules.

We then turned to formins. This family of actin NEPFs has been shown to distribute along microtubules (Thurston *et al.*, 2012) and to be independent of Arp2/3 for their NEPF activity. Incubation of the cells with the formin inhibitor small-molecule inhibitor of formin homology 2 (SMIFH2), which binds to formin homology FH2

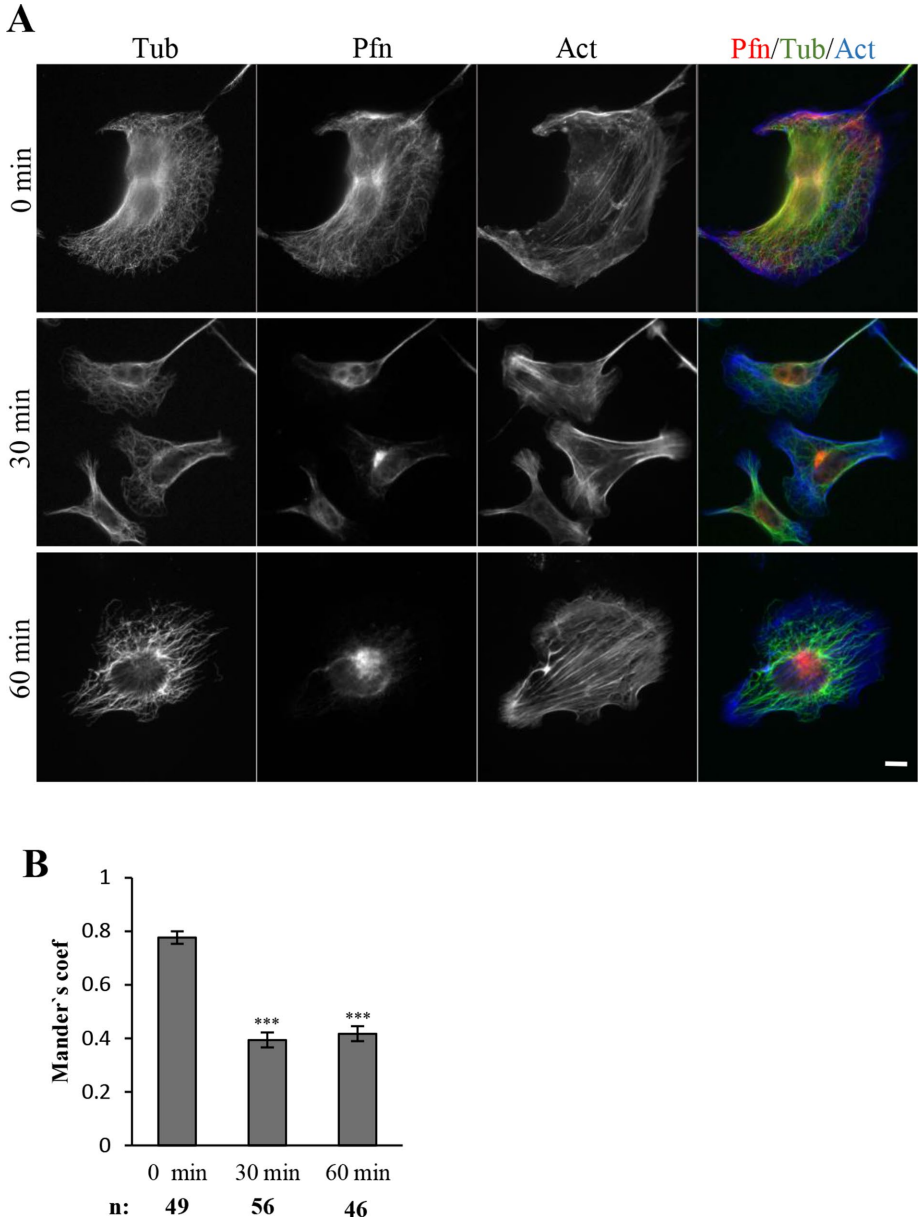

FIGURE 4: Increased lamellipodia formation decreases the profilin–microtubule codistribution. (A) B16 cells were treated with AlF_4 (see *Materials and Methods*) for 30 and 60 min, respectively, "demembranated" with Triton X-100, fixed, and stained for profilin, tubulin, and filamentous actin as in Figure 3. (B) Profilin–microtubule colocalization as in Figure 3. Three independent experiments; statistics as in Figure 1. Scale bar, 10 μm.

domains and interferes with their binding to both microtubules and filamentous actin (Rizvi *et al.*, 2009; Goldspink *et al.*, 2013), led to a significant decrease of the profilin codistribution with microtubules, strongly indicating that formins constitute a central component in recruitment of profilin/profilin-actin to microtubules (Figure 5). Of note in this context is that we kept the SMIFH2 exposure low (25 μM, 30 min) to avoid confounding effects, as reported by Isogai *et al.* (2015).

We further examined role of formins as profilin–microtubule linker molecules by siRNA down-regulation of Dia 1 and 2. Of these, the expression of Dia 2 is the least abundant in B16 cells (Block *et al.*, 2008). Reduced expression of either of the two isoforms separately did not result in a significant influence on the extent of profilin along the microtubules. However, by combining the two siRNAs and causing simultaneous down-regulation of both formins, we found a reduction in microtubule-associated profilin (Figure 5, C–E), in agreement with the result after the SMIFH2-exposure reported earlier. The reduced colocalization seen after combining the siRNAs was less extensive than after treatment with SMFH2, suggesting that other variants of formins may contribute to the microtubule recruitment of profilin.

On the basis of the foregoing results, we conclude that formins play a central role in distributing profilin to microtubules and this localization of profilin shifts with the activity status of the cell. The ability to associate with microtubules is shared by most formins, as is their profilin/profilin:actin–binding capacity, suggesting that the association of profilin to microtubules via formins is a general phenomenon; see later discussion.

Profilin affects microtubule growth dynamics

The view that microtubules control cell polarity and migration was put forward already in the 1970s (Vasiliev *et al.*, 1970), and in support of this conjecture, several studies have since reported on an intimate relationship between the microtubule and actin microfilament systems (see introduction and references in Coles and Bradke, 2015). Together with our aforementioned observations, this led us to assess whether profilin affected the organization of the microtubule array. We used siRNA to deplete profilin and analyzed two criteria for microtubule dynamics: α-tubulin acetylation and growth characteristics of microtubule ends. The former reflects microtubule stability; the longer individual polymers exist, the more their α-tubulin subunits become acetylated, which allowed us to use this posttranslational modification as a "timer" for microtubule turnover under control and profilin-depleted conditions.

Comparison of extracts from control cells with those transfected with profilin siRNA revealed a significant increase of acetylated α-tubulin in the latter (Figure 6 and Supplemental Figure S4). Analysis of the expression of histone deacetylase 6 and α-tubulin acetyltransferase, the principal enzymes responsible for tubulin deacetylation and acetylation, respectively, did not reveal any variation compared with cells transfected with control siRNA (unpublished data). We therefore conclude that cells expressing less profilin contain a larger fraction of long-lived microtubules.

To investigate whether modulating profilin expression had an effect on microtubule (+)-end growth, we transiently transfected cells with GFP-labeled EB3 protein in combination with control siRNA or profilin siRNA (Figure 7 and Supplemental Movies S1 and S2). Tracing >160 microtubule ends, respectively, in the two categories of transfected cells demonstrated that down-regulation of profilin expression increased microtubule growth rate 1.6 times. Reasoning

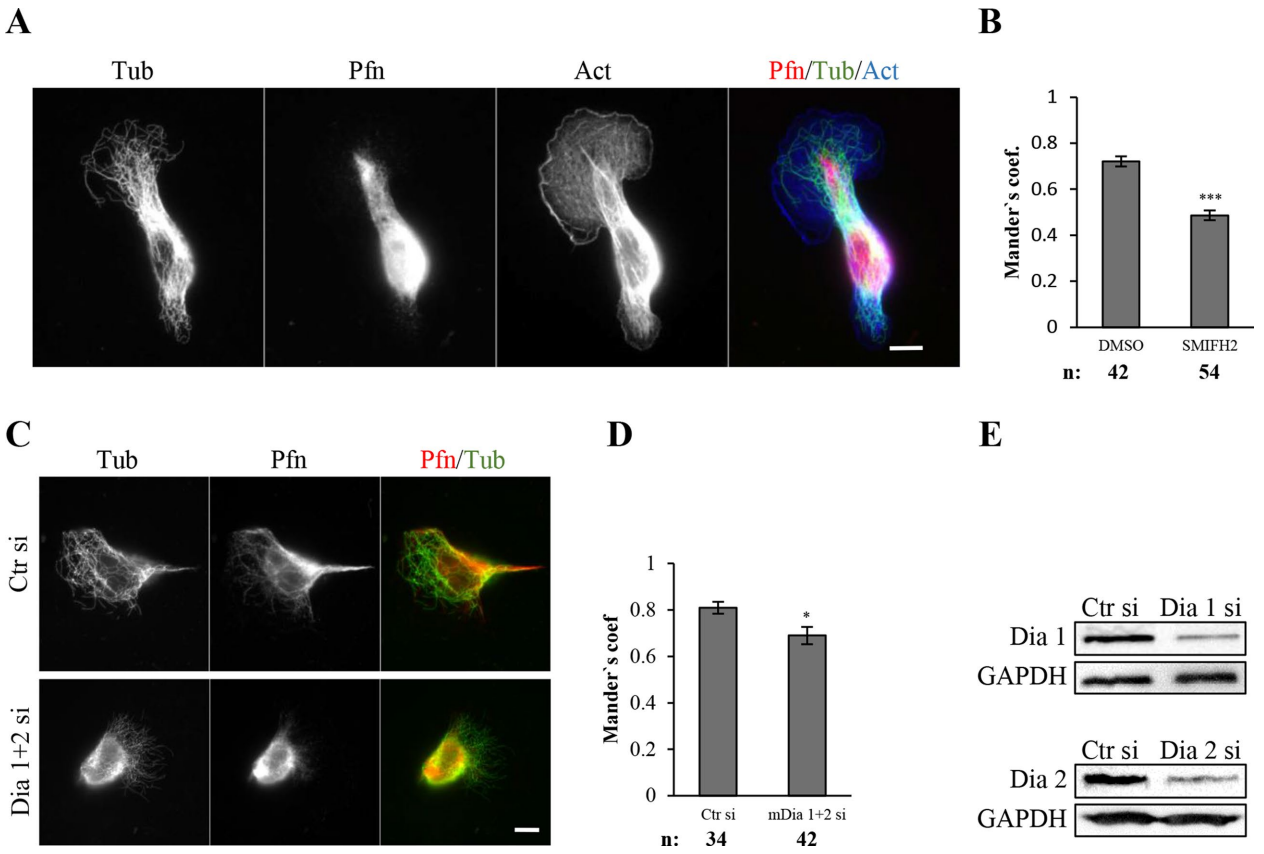

FIGURE 5: Formins are potential linkers between profilin and microtubules. (A) B16 cells were treated with the formin inhibitor SMIFH2 (25 µM) for 30 min; otherwise, conditions and labeling as in Figures 3 and 4. (B) Colocalization analysis. Two independent experiments; statistics as in Figure 1. (C) Cells after transfection with the control siRNA (top) and after transfection with pooled Dia 1 and 2 siRNAs (bottom) were fixed and stained for tubulin and profilin as before. (D) Quantitation of the colocalization of profilin and microtubules as in Figure 3. Two separate experiments; n = number of cells; statistics as in Figure 2. (E) Western blot showing reduced expression of mDia 1 and 2, respectively, after siRNA transfection; separate transfections of the two siRNAs. Scale bars, 10 µm.

that more rapidly growing microtubules might be reflected by a shorter distance between polymer ends and the leading edge of extending lamellipodia led us to measure this distance for >600 microtubules in ~40 cells (Figure 8). The result showed a major decrease of the distance between microtubule ends and lamellipodial tips; for control cells, 50% of the microtubules ended within 0.5 µm from the edge, whereas in cells expressing reduced amounts of profilin, this fraction increased to 80%, further underscoring the view that profilin plays a role in the control of microtubule growth.

In conclusion, down-regulation of profilin expression results in more long-lived microtubules that extend their (+)-end tips with increased speed toward the cell edge compared with cells under nonperturbed profilin conditions. Together, these experiments therefore suggest that under nondisturbed homeostatic growth, profilin increases microtubule dynamics by increasing the rate and/or frequency by which microtubules depolymerize from their (+)-ends. We conclude that profilin is not only a regulator of actin polymerization and a pivot, balancing different actin assembly forms, but it also has a role in the control of microtubule dynamics, affecting microtubule extension into the peripheral region of advancing cell edges.

DISCUSSION

Cell motility is a highly combinatorial phenomenon involving numerous signaling and force-generating processes by which the dynamically organized microtubule and microfilament systems function as ultimate and coordinated generators of directional force (Pollard and Borisy, 2003; Rodriguez *et al.*, 2003; Field and Lenart, 2011). Here we provide evidence that profilin, a central control

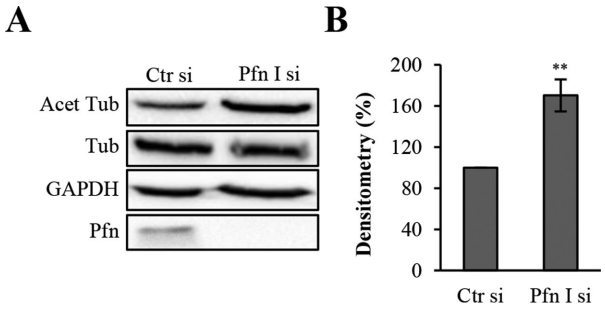

FIGURE 6: Down-regulation of profilin expression increases acetylation of tubulin. (A) Cells were transfected with control siRNA (Ctr si) or a cocktail of four different profilin I siRNAs (Pfn I si), and resulting extracts were analyzed by Western blot for the presence of acetylated tubulin (Acet Tub), tubulin, glyceraldehyde phosphate dehydrogenase (GAPDH; loading control), and profilin. (B) Quantification of blotted bands by densitometry; mean value of four independent experiments. Statistics as in Figure 1; $^{**}p \leq 0.01$.

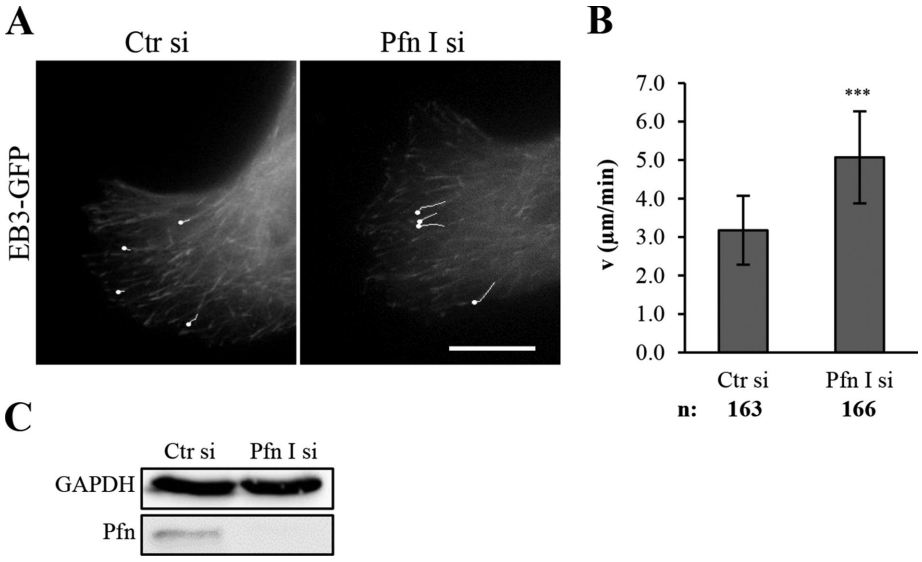

FIGURE 7: Profilin influences microtubule dynamics. (A) Video clips (Supplemental Videos S1 and S2) at 5-s intervals of EB3-GFP–transfected B16 cells after subsequent transfection with control siRNA or Pfn I siRNA (left and right, respectively). Traces of the advancement of some microtubule plus ends over a period of 15 s are indicated. Note the longer distances after down-regulation of profilin expression, which correspond to increased microtubule growth velocity as shown in B. Only cells positive for siGloRNA, indicating siRNA transfection, were selected for the measurements. The microtubule (+)-end growth rate was established by frame-by-frame analysis of the videos to ensure measurement of uninterrupted extension solely. Three independent experiments; six cells (two from each); *n* = number of microtubule plus ends (similar number per cell and experiment). Statistics as in Figure 1. Scale bar, 10 µm. (C) Cell cultures used for live-cell imaging were lysed and analyzed by Western blot to verify reduced profilin expression.

component of actin assembly, well known as a regulator of actin polymerization (Carlsson *et al.*, 1977; reviewed by (Witke, 2004; Jockusch *et al.*, 2007; Karlsson and Lindberg, 2007) and recently proposed to balance different NEPF-driven filament assembly formations (Rotty *et al.*, 2015; Suarez *et al.*, 2015) and coordinate filament barbed-end growth (Pernier *et al.*, 2016; Shekhar *et al.*, 2016), also is linked to the control of microtubule dynamics via an indirect interaction mediated by formins.

That a thoroughly characterized protein such as profilin, which has been studied since the 1970s, now is found to distribute to the discrete and easily recognized microtubule array in cultured cells may appear unexpected. However, a retrospective scrutiny of earlier localization studies of profilin by fluorescence microscopy from other laboratories (Buss *et al.*, 1992; Mayboroda *et al.*, 1997), as well as from our published work (Hájková, 1999; Skare *et al.*, 2003), reveals that such a microtubule localization was hinted at long before we reported that profilin indeed partially codistributes with microtubules in human fibroblasts (Grenklo *et al.*, 2004). More recently, this was confirmed by Bender *et al.* (2014), who detected a codistribution of profilin with microtubules in platelets and fibroblasts and, in agreement with our observations here, observed an increased microtubule acetylation in profilin-deficient platelets. The reason that the connection of profilin to microtubules was not generally acknowledged before is probably due to the random profilin distribution observed by standard fluorescence microscopy of cultured cells (see *Introduction*) together with the strong bias for profilin as a major actin regulator, as demonstrated for a range of cell types (Carlsson *et al.*, 1977; Lassing and Lindberg, 1988; Ballweber *et al.*, 1998; Kaiser *et al.*, 1999; Hajkova

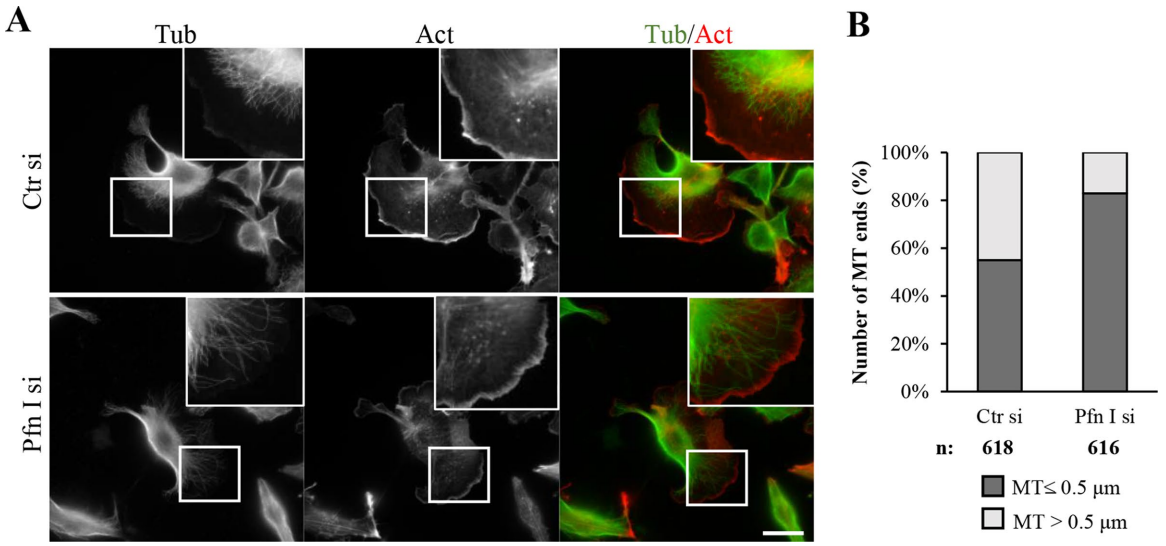

FIGURE 8: Microtubule ends reach closer to the cell edge after down-regulation of profilin. (A) The B16 cells were transfected with control siRNA or profilin I siRNA and stained with tubulin antibodies and rhodamine-phalloidin. The distance between the microtubule ends and the cell edge, defined as the outermost rhodamine staining of the lamellipodia, was measured by SlideBook software (see *Materials and Methods*). (B) Number of microtubules that end within 0.5 µm (dark gray) or at a longer distance from the edge (light gray), respectively. Two independent experiments, ~40 cells; *n* = number of microtubules. Scale bar, 10 µm.

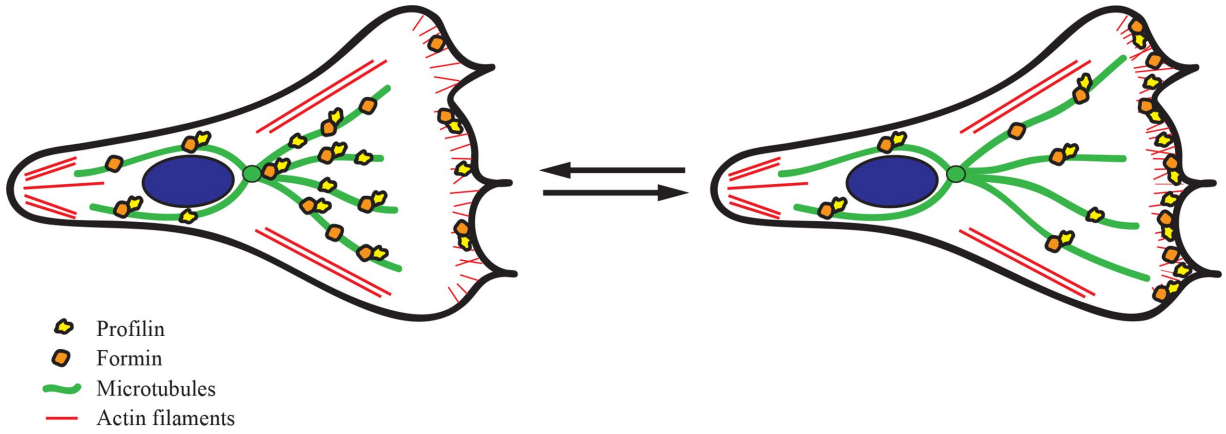

FIGURE 9: Model of profilin function in relation to microtubules based on the present data. During homeostatic growth and motility, the presence of profilin (yellow) along microtubules (green) is balanced against the requirement for its documented role as a regulator of actin polymerization. Formins (orange) are major profilin-recruiting components on the microtubules, as indicated by experiments with SMIFH2 and siRNA. In addition, formins and profilin are found at the cell periphery, where they participate in actin regulation. Interfering with actin dynamics as with CytD and Jasp (see the text) causes accumulation of profilin to microtubules, as also reported for formins (Bartolini *et al.*, 2012). Depletion of microtubule-associated profilin after siRNA transfection results in faster growth of microtubules and increased acetylation of tubulin. Similarly, stimulation of actin dynamics by AlF_4 reduced profilin association along the microtubules and increased tubulin acetylation and lamellipodia formation. We hypothesize a similar scenario in response to increased receptor activation. At the periphery, profilin cooperates with formins and other actin NEPFs for rapid elongation of the submembranous actin array and advancement of the cell front. The increased microtubule growth in the direction of the forward-moving membrane allows for increased microtubule-dependent transport in support of the advancing edge. Our observations as summarized by this model therefore identify profilin as part of a molecular network that coordinates actin and microtubule functions in migrating cells.

et al., 2000; Lu and Pollard, 2001; Grenklo *et al.*, 2003), including platelets (Markey *et al.*, 1981). To our knowledge, the data presented here are the first evidence that profilin plays a role in controlling microtubule growth dynamics and hence contributes to the coordination of the actin and microtubule systems; see model in Figure 9.

We could not connect the microtubule-associated and WASP-related protein WHAMM with the profilin-microtubule interaction. Like other WASP-family proteins, WHAMM is an Arp2/3-dependent NEPF; it has been suggested to cause intracellular membrane modulation and trafficking between endoplasmic reticulum (ER) and Golgi (Campellone *et al.*, 2008), and recently was linked to autophagosome biogenesis via nucleation and formation of an ER-tethered actin comet tail–like assembly process (Kast *et al.*, 2015). Here we showed that profilin binds a WHAMM fragment, which contains a polyproline sequence motif typically known to recruit profilin/profilin:actin (Bjorkegren *et al.*, 1993) and to be essential for efficient profilin:actin–dependent filament growth (e.g., Lu and Pollard, 2001; Yarar *et al.*, 2002; Grenklo *et al.*, 2003). Given the collective results, this makes WHAMM an ideal candidate as a connecting molecule between profilin and microtubules, and we cannot unequivocally exclude that it has such a function, for instance, in the Golgi region (Dong *et al.*, 2000) or other similarly confined areas of the cell.

In contrast, our data identify microtubule-associated formins as major profilin/profilin:actin–recruiting components. The ability to associate with microtubules is shared by most formins and occurs via their FH2 domain (Bartolini *et al.*, 2008, 2012; Thurston *et al.*, 2012). Similarly, their capacity to bind profilin/profilin:actin is common among them and depends on their FH1 domain, which contains a polyproline sequence. Hence the formins are central actin NEPFs along with the WASP/WAVE and Ena/VASP families of proteins. Among the formins, Dia 1 and 2 have a special role in the context of microtubules since in addition to their association along the polymers, they have been identified as binding partners to the APC protein (Bartolini and Gundersen, 2010; Okada *et al.*, 2010), a component of the +TIP complex controlling the (+)-end of microtubules. Furthermore, APC has been shown to cooperate with Dia to induce rapid actin polymerization from profilin:actin. Hence formin–microtubule interactions can occur both directly via interactions along the polymer and indirectly via +TIPs.

The distribution of profilin along the microtubules is in agreement with the view that actin polymerization contributes to membrane tubulation along microtubules (Campellone *et al.*, 2008); in fact, the profilin we detect along microtubules may represent profilin:actin as much as profilin alone. Not least, the differential effect of the drug treatments and motility up-regulation by AlF4 suggest that profilin:actin contributes to this pool of profilin. Observations that formins affect microtubule stability in NIH 3T3 fibroblasts (Bartolini *et al.*, 2012; Thurston *et al.*, 2012) and of increased Dia 1 association with microtubules after treatment with latrunculin (Bartolini *et al.*, 2012), which interferes with actin polymerization and causes derangement of filamentous actin, are in agreement with the results presented here. We show that reducing actin dynamics by CytD and Jasp causes profilin/profilin:actin to accumulate along the microtubules. Furthermore, in support of cooperation with microtubule-associated formins, we observe an influence of profilin on microtubule stability. Together these observations point to a scenario in which microtubule-associated and -stabilizing formins recruit profilin and profilin:actin to the polymer. In this situation, the polymer-stabilizing effect of the formin is balanced by its engagement as an actin NEPF at actin filament barbed ends generated in the vicinity. This, in turn, depends on the availability of profilin:actin. Hence, when less profilin is expressed, more formin

molecules remain microtubule associated, as reflected in more stable polymers, as seen here.

It is also possible that some of the profilin molecules derive from translation of microtubule-associated profilin mRNA (Johnsson and Karlsson, 2010), similar to what has been reported for the intermediary protein peripherin (Chang *et al.*, 2006). The extent to which microtubules serve as platforms for actin-driven membrane modulations is likely to vary with conditions and cell type. For instance, in platelets, as reported by Bender *et al.* (2014), the association of profilin/profilin:actin with microtubules seems to serve as a localized reservoir for actin in a polymerization-ready form from which actin is recruited for the massive filament formation typically seen upon platelet activation (Markey *et al.*, 1981; Karlsson *et al.*, 1984).

Clearly, our observation that profilin plays a role in controlling the dynamics of microtubule ends is difficult to reconcile with its presence along the entire polymer length. As discussed, we saw that reducing profilin expression by siRNA increased tubulin acetylation, which is indicative of more stable microtubules, and by imaging cells transfected with EB3-GFP, we saw increased microtubule growth after reduced profilin concentration. Congruent with this, we also measured a smaller average distance between the cell edge and microtubule tips that extended toward lamellipodia, in the direction of edge advancement. Collectively this means that under nonperturbed conditions, profilin reduces microtubule growth by contributing to the frequency and/or pausing by which microtubule (+)-ends undergo catastrophe (see model in Figure 9). Such scenarios would result from lowering the rate of addition of new GTP-charged α/β-tubulin subunits. Possibly profilin combines with +TIP-interacting formins (Okada *et al.*, 2010) to have such a function in parallel to its "gatekeeping" role to direct formation of different actin assembly forms (Henty-Ridilla and Goode, 2015). It cannot be excluded that the increased microtubule dynamics observed in profilin-depleted cells was due to a general derangement of the microfilament system, resulting in less-confined space for microtubule growth. However, on the basis of our microscopy analysis, we consider this unlikely, since lamellipodia formation and phalloidin staining remained largely unperturbed over the time frame when the measurements were performed. Moreover, for the live-cell imaging, we selected cells of wild-type morphology with clearly recognizable lamellipodia and in which individual microtubules could be identified and their elongation measured.

Microtubule (+)-ends have been implicated in focal adhesion turnover (Krylyshkina *et al.*, 2003), and our data show that profilin contributes to the capacity of microtubule ends to probe advancing lamellae by increasing their turnover in migrating cells. Clearly, there is much more to understand concerning profilin function in this context.

MATERIALS AND METHODS

Cell culturing

Mouse melanoma B16-F1 and HEK293T cells were cultured in DMEM (Thermo Scientific, Stockholm, Sweden) supplemented with 10% fetal calf serum (FCS) at 37°C in the presence of 5% CO_2.

Antibodies

Antibodies used were as follows: against α-tubulin, from Abcam (Cambridge, UK), ab7291 and ab18251, made in mouse and rabbits, respectively (used at dilutions of 1:2000 for Western blot and 1:200 for microscopy); against Dia 1 (1:1000), ab1173; against glyceraldehyde phosphate dehydrogenase, ab8245 (1:40,000); against kinesin, K1005 (1:50); against Ac-tubulin, T6793 (1:500); against the profilin I N-terminal, P7749 (1:100); and against β-actin, A5441 (1:4000), from Sigma-Aldrich, Stockholm, Sweden; against profilin I (our laboratory, raised in rabbits, 1:2000); against β-arrestin, from Santa Cruz Biotechnology (Heidelberg, Germany), against Dia 2, sc9182 (1:20) and sc-393499 (1:100); against GFP, from Roche (Stockholm, Sweden), 11814460001 (1:2000); horseradish peroxidase (HRP) conjugated against mouse immunoglobulin (Ig), from Dako (Stockholm, Sweden), P0447 (1:2000); against rabbit Ig, from Pierce (Stockholm, Sweden), 1858415 (1:1000); fluorescein isothiocyanate (FITC) conjugated against mouse and rabbit Ig, from Jackson ImmunoResearch Laboratories (West Grove, PA), 705-095-003 (1:400) and 711-095-152 (1:1000), respectively; and tetramethylrhodamine isothiocyanate conjugated against rabbit Ig, from Thermo Fisher Scientific (Stockholm, Sweden), 115-025-062 (1:400).

siRNA transfection and Western blot analysis

B16 cells were transfected with a siRNA cocktail of four different profilin siRNA duplexes (50 nM each, LQ-062705-01; Dharmacon (Stockholm, Sweden); for sequences, see Supplemental Figure S4) or a nontargeting control siRNA (D-001910-03; Dharmacon) using Lipofectamine 2000 (Invitrogen, Stockholm, Sweden). Dia 1 and 2 siRNAs were from Santa Cruz Biotechnology, sc-35191 and sc-155883, respectively. For transfections, 25 nM of each was used. The cells were lysed after 24 h in Passive Lysis Buffer (31655601; Promega, Stockholm, Sweden) unless otherwise stated, and the protein concentration was determined by Bradford protein assay. After SDS–PAGE electrophoresis, the separated proteins were transferred to a nitrocellulose membrane (Hybond-C Extra; Amersham Bioscience, Uppsala, Sweden) and identified by primary antibodies and HRP-conjugated secondary antibodies. The membranes were developed using West Dura HRP substrate (Pierce). Images were captured on a ChemiDoc (Bio-Rad, Stockholm, Sweden) using Quantity One software for densitometry.

Microtubule-partitioning assay

B16 cells cultured overnight were trypsinized (Thermo Scientific) and suspended in DMEM (Life Technologies, Stockholm, Sweden) supplemented with 10% FCS. After adjustment to a final concentration of 2×10^6 cells/ml, they were treated with either 35 μM Taxol (paclitaxel, T7402; Sigma-Aldrich) for 4 min at 37°C or 66 μM nocodazole (74151; Fluka, Stockholm, Sweden) for 15 min at 37°C and then centrifuged at 1200 × *g* in an Eppendorf centrifuge for 30 s. The pelleted cells were resuspended in 200 μl of PEM buffer (80 mM 1,4-piperazinediethanesulfonic acid [PIPES], pH 6.9, 5 mM ethylene glycol tetraacetic acid [EGTA], 1 mM $MgCl_2$) supplemented with 0.5% Triton X-100 and 5 μl/ml leupeptin (L0649; Sigma-Aldrich). The extracts were centrifuged at 1800 × *g* for 30 s, the resulting pellets stocked at –20°C, and the supernatants precipitated with acetone overnight at –20°C. Subsequently the precipitated supernatant material was collected by centrifugation, resuspended in 200 μl of SDS–PAGE sample buffer, and boiled immediately in parallel with the original pellet material after similar sample preparation and volume adjustment to allow for direct comparison of the two fractions.

Coimmunoprecipitation

B16 cells transfected with either pEGFP C1 or citrine-profilin (CTN-Pfn) encoding enhanced GFP (EGFP) or CTN-Pfn, respectively, were lysed in 200 μl of 20 mM Tris-HCl, pH 6.9, plus 0.5% NP-40, 2 M glycerol, 10% dimethyl sulfoxide (DMSO), 1 mM $MgCl_2$, 2 mM EGTA, 200 μM sodium orthovanadate, 5 μg/μl leupeptin, and 500 μM phenylmethylsulfonyl fluoride (Wersinger and Sidhu, 2005). The cell extracts were centrifuged at 10,000 × *g* for 5 min, and 50 μl of the supernatant was boiled in SDS–PAGE sample buffer and saved as control (input), with the remaining extract volume precleared with 40 μl of Sepharose 4B (50% slurry; 51-1870-04;

Pharmacia Fine Chemicals, Stockholm, Sweden) for 30 min and then incubated with 40 µl of Nanobody^{GFP}-beads (camelid antibodies against GFP; e.g., Kirchhofer *et al.*, 2010) coupled to *N*-hydroxysuccinimide–activated agarose (26200; Pierce) as described by Holmberg *et al.* (2014). After incubation, the beads were washed four times with buffer before being boiled in 60 µl of SDS–PAGE sample buffer and loaded onto an SDS page.

GST-fusion protein purification and pull-down assay

GST-WHAMM/CC (amino acid residues 559–809), GST-WASP/VCA (amino acid residues 442-502), and GST alone were expressed in *E. coli* and purified using glutathione-Sepharose beads (GE Healthcare, Uppsala, Sweden). For the GST pull down with GST-WHAMM and GST-WASP, HEK293T cells were lysed in 10 mM Tris HCl, pH 7.5, 0.5% Triton X-100, 10% glycerol, 100 mM NaCl, and 1% aprotinin (lysis buffer). The cell lysates were centrifuged at 13,000 rpm in a bench-top microcentrifuge for 15 min at 4°C. The supernatant was collected and incubated with the pretreated beads for 60 min end over end at 4°C. The beads were washed three times with lysis buffer and then analyzed by SDS–PAGE and electrotransferred to nitrocellulose filters (GE Healthcare).

Citrine-profilin fusion construct

Citrine was PCR amplified from plasmid pRSETb-Citrine (a generous gift from Roger Tsien, University of California, San Diego) using primers containing a restriction site for *Pst*I and encoding linker residues (forward, TAT CTG CAG TCT GGG TCT AGT GGT TCT CTG CAG TCT GGG TCT AGT; reverse, ATC CTG CAG TGA CCC GCC CTG CAG TGA CCC GCC), gel purified, and digested with *Pst*I. The human profilin cDNA (Pfn1; Gene ID 5216) was introduced into pEGFPc2 (GenBank accession number U57606; Clontech, Saint-Germain-en-Laye, France), followed by excision of the EGFP gene, religation, and subsequent *Pst*I cleavage. The gel-purified and *Pst*I-digested citrine cDNA was then ligated into the opened profilin gene in the pc2 vector to generate the internal fusion gene encoding the CTN-Pfn, where the citrine C- and N-termini are fused via linker residues to Q79 and D80, respectively, in profilin. The object with this construct was to avoid linking the fluorophore protein to the amino or carboxy terminus of profilin since these positions may interfere with profilin's interaction with poly-L-proline (Wittenmayer *et al.*, 2000). As sought for, CTN-Pfn retains full binding capacity for poly-L-proline, whereas its interaction with actin is reduced. The in vitro characterization of CTN-Pfn will be published elsewhere (Nejedla, Masser, Li, Biancospino, Spiess, and Karlsson, unpublished data).

Microtubule protein preparation, cosedimentation, and assembly assays

For details, see Draberova *et al.* (2010). Briefly, porcine brain tubulin and thermostable microtubule-associated proteins (MAPs) containing MAP2 and tau were isolated from microtubule protein (MTP-2). For cosedimentation, Taxol-stabilized microtubules (6 µM tubulin) were mixed with profilin, MAPs, or bovine serum albumin (final concentrations 0.10–0.13 mg/ml) and incubated for 30 min at 37°C. The mixture (120 µl) was centrifuged for 20 min at 25°C on a 4 M glycerol cushion (800 µl) in 80 mM PIPES, pH 6.8, 1 mM EGTA, and 1 mM $MgCl_2$ containing 10 µM Taxol in an MLS50 rotor (Beckman Coulter, Fullerton, CA) at 43,000 rpm. The protein content of the starting mixtures, supernatants, and pellets was resolved on 12.5% SDS–PAGE. Pellets were resuspended in sample buffer that equaled 0.5 times the supernatant volume. The tubulin assembly was monitored by turbidimetry at 350 nm and 37°C for samples containing 20 µM tubulin in 80 mM PIPES, pH 6.8, 1 mM EGTA, 1 mM $MgCl_2$, 1 mM GTP, and 3.0 M glycerol plus 20 µl of profilin (25 µM final concentration) in 10 mM NaCl, 5 mM Tris, pH 7.8, and 10% glycerol. The final sample volume was 100 µl. Control samples contained 20 µl of thermostable MAPs (1.91 mg/ml) or the profilin buffer alone.

Proximity ligation assay and fluorescence microscopy

B16 cells cultured on coverslips precoated with 25 µg/ml laminin (L2020; Sigma-Aldrich) for 2 h at 37°C were fixed for 20 min at 37°C with 4% formaldehyde (Sigma-Aldrich) in phosphate-buffered saline (PBS) containing 5 mM EGTA and then demembranated with 0.1% Triton X-100 in PBS-EGTA for 10 min at room temperature. The PLA was carried out using the Duolink PLA in situ kit (Olink Biosciences, Uppsala, Sweden) following the manufacturer's protocol. The cells were incubated with primary avian antibodies generated against cross-linked profilin:actin (Nyman *et al.*, 2002a) and affinity purified on immobilized actin and profilin, respectively (previously referred to as AI, AII, PI, and PII, where the roman numeral indicates two different animals immunized as described in Grenklo *et al.*, 2004; Li *et al.*, 2008). Together with these profilin/profilin:actin antibodies used at a concentration of 50 µg/ml, anti–α-tubulin (generated in mice), anti–α-tubulin (rabbit), anti-kinesin, and anti-β-arrestin were added for 1 h at room temperature, followed by incubation with species-specific secondary antibodies conjugated with oligonucleotides (PLA probes MINUS and PLUS). To allow for visualization of microtubules simultaneously with the PLA signal, the buffer solution containing fluorescent oligonucleotides was supplemented with a FITC-labeled secondary antibody recognizing rabbit anti-tubulin. The coverslips were mounted in ProLong Gold (Molecular Probes, Stockholm, Sweden), and microscopy was performed using a Leica DMLB microscope equipped with 63×/1.32 objective lens and a DC350F charge-coupled device camera (Leica Microsystems, Stockholm, Sweden). To compare signal density among different samples, four representative areas were selected per cell in each experiment: two in lamellipodia and two in the center of the lamella, each a circle of 6.6 µm^2. The number of distinct dots in these was determined, and mean values obtained by the different PLA labelings were compared.

To visualize profilin distribution along microtubules by fluorescence microscopy, B16 cells were cultured on coverslips, washed with PBS, and permeabilized for 40 s in PEM buffer containing 0.5% Triton X-100 before fixation for 20 min in PEM containing 1% DMSO and 3.7% formaldehyde (Raynaud-Messina *et al.*, 2004; Bouissou *et al.*, 2009). Drug treatment as indicated was performed before permeabilization with 0.1% DMSO (vehicle), 0.5 µM CytD, 0.05 µM Jasp, 25 µM SMIFH2, and 50 µM CK-666 for 30 min or with a mixture of 50 µM $AlCl_3$ and 30 mM NaF for 30 and 60 min to generate AlF_4. The samples were then incubated with SiR-actin (SC001; Tebu-Bio, Roskilde, Denmark), primary and secondary antibodies as indicated, mounted, and observed using an Axiovert 200 M fluorescence microscope (Carl Zeiss, Stockholm, Sweden) equipped with a climate chamber, an EC-Plan-Neofluar 63×/1.4 objective lens, and a DG-4 light source (Sutter Instrument, Spänga, Sweden). Images were captured with a Cascade 1K camera (Roper, Stockholm, Sweden). Profilin–microtubule codistribution in leading lamellae was quantified using the ImageJ plug-in image correlation analysis (Manders colocalization coefficient). SlideBook software was used to measure the distances between microtubule ends and outer edges of the lamellipodia by drawing a straight line from each microtubule end to the edge, which was marked by rhodamine-phalloidin (1:200; P1951; Sigma-Aldrich).

Live-cell imaging of EB3-GFP–transfected cells

B16 cells were cultured on laminin-coated glass-bottom dishes (P35GC-1.5-10-C; MatTek, Ashland, MA). After 24 h, the cells were

transfected with 20 ng/µl EB3-GFP, 5 nM siGloRNA (D-001630-02; Dharmacon), and siRNA cocktail (as described earlier) and cultured for an additional 24 h. Then cells expressing siGloRNA were identified for EB3-GFP recording at 37°C in the presence of 5% CO_2, using the same microscope and settings as for fluorescence microscopy. Images were acquired at 5-s intervals during 5-min periods.

TIRF microscopy

Cells transiently expressing the citrine-profilin fusion were culture on glass as for live imaging and fixed with formaldehyde. After detergent demembranation and labeling with tubulin antibodies, they were observed in TIRF mode with a AxioObserver D1 Laser TIRF 3 system (Carl Zeiss) equipped with an alpha Plan-Apochromat 63×/1.46 oil objective lens, optically pumped semiconductor (488 nm/20 mW) and diode-pumped solid-state (561 nm/20 mW) lasers, and 52HE (488 nm) and 86HE (561 nm) shift-free filter sets. Images were captured with an AxioCam MRm rev.3 camera (Carl Zeiss), and the system was controlled by ZEN blue 2011 software.

Superresolution multicolor imaging

STED was performed with a Leica TCS SP8 3X STED microscope equipped with a 100×/1.4 STED WHITE objective. Optimal excitation wavelengths were selected from a broadband white-light fiber laser source (tunable range 470–670 nm). Stimulated emission depletion was performed with a high-power fiber laser at 775 nm that achieves a lateral resolution of <50 nm.

ACKNOWLEDGMENTS

We thank Martin Gullberg (Umeå University, Umeå, Sweden) and Mikael Sellin (ETH Zurich, Zurich, Switzerland) for fruitful discussions concerning the microtubule-partitioning assay, Olle Larsson (Karolinska Institute, Stockholm, Sweden) for generously providing the β-arrestin antibody, and Robert Grosse (University of Marburg, Marburg, Germany) for the EB3-GFP–expressing plasmid. All microscopy except STED was performed with excellent support at the Imaging Facility of Stockholm University. Financial support from the Foundation Olle Enkvist Byggmästare and the Carl Trygger Foundation to R.K., the Swedish Cancer Society to P.A., and the Czech Republic Grant Agency to P.D. is gratefully acknowledged.

REFERENCES

Akhmanova A, Steinmetz MO (2008). Tracking the ends: a dynamic protein network controls the fate of microtubule tips. Nat Rev Mol Cell Biol 9, 309–322.

Ballweber E, Giehl K, Hannappel E, Huff T, Jockusch BM, Mannherz HG (1998). Plant profilin induces actin polymerization from actin : beta-thymosin complexes and competes directly with beta-thymosins and with negative co-operativity with DNase I for binding to actin. FEBS Lett 425, 251–255.

Bartolini F, Gundersen GG (2010). Formins and microtubules. Biochim Biophys Acta 1803, 164–173.

Bartolini F, Moseley JB, Schmoranzer J, Cassimeris L, Goode BL, Gundersen GG (2008). The formin mDia2 stabilizes microtubules independently of its actin nucleation activity. J Cell Biol 181, 523–536.

Bartolini F, Ramalingam N, Gundersen GG (2012). Actin-capping protein promotes microtubule stability by antagonizing the actin activity of mDia1. Mol Biol Cell 23, 4032–4040.

Bender M, Stritt S, Nurden P, van Eeuwijk JM, Zieger B, Kentouche K, Schulze H, Morbach H, Stegner D, Heinze KG, *et al*. (2014). Megakaryocyte-specific Profilin1-deficiency alters microtubule stability and causes a Wiskott-Aldrich syndrome-like platelet defect. Nat Commun 5, 4746.

Bertling E, Quintero-Monzon O, Mattila PK, Goode BL, Lappalainen P (2007). Mechanism and biological role of profilin-Srv2/CAP interaction. J Cell Sci 120, 1225–1234.

Bjorkegren C, Rozycki M, Schutt CE, Lindberg U, Karlsson R (1993). Mutagenesis of human profilin locates its poly(L-proline)-binding site to a hydrophobic patch of aromatic amino acids. FEBS Lett 333, 123–126.

Block J, Stradal TE, Hanisch J, Geffers R, Kostler SA, Urban E, Small JV, Rottner K, Faix J (2008). Filopodia formation induced by active mDia2/Drf3. J Microsc 231, 506–517.

Blom M, Reis K, Nehru V, Blom H, Gad AK, Aspenstrom P (2015). RhoD is a Golgi component with a role in anterograde protein transport from the ER to the plasma membrane. Exp Cell Res 333, 208–219.

Bouissou A, Verollet C, Sousa A, Sampaio P, Wright M, Sunkel CE, Merdes A, Raynaud-Messina B (2009). γ-Tubulin ring complexes regulate microtubule plus end dynamics. J Cell Biol 187, 327–334.

Bugyi B, Carlier MF (2010). Control of actin filament treadmilling in cell motility. Annu Rev Biophys 39, 449–470.

Buss F, Temm-Grove C, Henning S, Jockusch BM (1992). Distribution of profilin in fibroblasts correlates with the presence of highly dynamic actin filaments. Cell Motil Cytoskeleton 22, 51–61.

Campellone KG, Webb NJ, Znameroski EA, Welch MD (2008). WHAMM is an Arp2/3 complex activator that binds microtubules and functions in ER to Golgi transport. Cell 134, 148–161.

Carlsson L, Nystrom LE, Sundkvist I, Markey F, Lindberg U (1977). Actin polymerizability is influenced by profilin, a low molecular weight protein in non-muscle cells. J Mol Biol 115, 465–483.

Chang L, Shav-Tal Y, Trcek T, Singer RH, Goldman RD (2006). Assembling an intermediate filament network by dynamic cotranslation. J Cell Biol 172, 747–758.

Chaudhry F, Little K, Talarico L, Quintero-Monzon O, Goode BL (2010)A central role for the WH2 domain of Srv2/CAP in recharging actin monomers to drive actin turnover in vitro and in vivo. Cytoskeleton (Hoboken) 67, 120–133.

Chesarone MA, DuPage AG, Goode BL (2010). Unleashing formins to remodel the actin and microtubule cytoskeletons. Nat Rev Mol Cell Biol 11, 62–74.

Coles CH, Bradke F (2015). Coordinating neuronal actin-microtubule dynamics. Curr Biol 25, R677–R691.

Dong J, Radau B, Otto A, Muller E, Lindschau C, Westermann P (2000). Profilin I attached to the Golgi is required for the formation of constitutive transport vesicles at the trans-Golgi network. Biochim Biophys Acta 1497, 253–260.

Draberova E, Sulimenko V, Sulimenko T, Bohm KJ, Draber P (2010). Recovery of tubulin functions after freeze-drying in the presence of trehalose. Anal Biochem 397, 67–72.

Dunn KW, Kamocka MM, McDonald JH (2011). A practical guide to evaluating colocalization in biological microscopy. Am J Physiol Cell Physiol 300, C723–742.

Field CM, Lenart P (2011). Bulk cytoplasmic actin and its functions in meiosis and mitosis. Curr Biol 21, R825–830.

Gad AK, Nehru V, Ruusala A, Aspenstrom P (2012). RhoD regulates cytoskeletal dynamics via the actin nucleation-promoting factor WASp homologue associated with actin Golgi membranes and microtubules. Mol Biol Cell 23, 4807–4819.

Goldspink DA, Gadsby JR, Bellett G, Keynton J, Tyrrell BJ, Lund EK, Powell PP, Thomas P, Mogensen MM (2013). The microtubule end-binding protein EB2 is a central regulator of microtubule reorganisation in apico-basal epithelial differentiation. J Cell Sci 126, 4000–4014.

Grantham J, Lassing I, Karlsson R (2012). Controlling the cortical actin motor. Protoplasma 249, 1001–1015.

Grenklo S, Geese M, Lindberg U, Wehland J, Karlsson R, Sechi AS (2003). A crucial role for profilin-actin in the intracellular motility of Listeria monocytogenes. EMBO Rep 4, 523–529.

Grenklo S, Johansson T, Bertilson L, Karlsson R (2004). Anti-actin antibodies generated against profilin:actin distinguish between non-filamentous and filamentous actin, and label cultured cells in a dotted pattern. Eur J Cell Biol 83, 413–423.

Gupta KK, Alberico EO, Nathke IS, Goodson HV (2014). Promoting microtubule assembly: a hypothesis for the functional significance of the +TIP network. Bioessays 36, 818–826.

Hahne P, Sechi A, Benesch S, Small JV (2001). Scar/WAVE is localised at the tips of protruding lamellipodia in living cells. FEBS Lett 492, 215–220.

Hájková L (1999). The Dynamic Microfilament System. PhD Thesis. Stockholm, Sweden: Stockholm University.

Hajkova L, Nyman T, Lindberg U, Karlsson R (2000). Effects of cross-linked profilin:beta/gamma-actin on the dynamics of the microfilament system in cultured cells. Exp Cell Res 256, 112–121.

Henty-Ridilla JL, Goode BL (2015). Global resource distribution: allocation of actin building blocks by profilin. Dev Cell 32, 5–6.

Holmberg MA, Gowda NK, Andreasson C (2014). A versatile bacterial expression vector designed for single-step cloning of multiple DNA fragments using homologous recombination. Protein Expr Purif 98, 38–45.
Isogai T, van der Kammen R, Innocenti M (2015). SMIFH2 has effects on Formins and p53 that perturb the cell cytoskeleton. Sci Rep 5, 9802.
Jockusch BM, Murk K, Rothkegel M (2007). The profile of profilins. Rev Physiol Biochem Pharmacol 159, 131–149.
Johnsson AK, Karlsson R (2010). Microtubule-dependent localization of profilin I mRNA to actin polymerization sites in serum-stimulated cells. Eur J Cell Biol 89, 394–401.
Kaiser DA, Vinson VK, Murphy DB, Pollard TD (1999). Profilin is predominantly associated with monomeric actin in Acanthamoeba. J Cell Sci 112, 3779–3790.
Karlsson R, Lassing I, Hoglund AS, Lindberg U (1984). The organization of microfilaments in spreading platelets: a comparison with fibroblasts and glial cells. J Cell Physiol 121, 96–113.
Karlsson R, Lindberg U (2007). Profilin, an essential control element for actin polymerization. In: Actin-Monomer-Binding Proteins, ed. P Lappalainen, New York: Springer/Landes Bioscience, 29–44.
Kast DJ, Zajac AL, Holzbaur EL, Ostap EM, Dominguez R (2015). WHAMM directs the Arp2/3 complex to the ER for autophagosome biogenesis through an actin comet tail mechanism. Curr Biol 25, 1791–1797.
Kaverina I, Rottner K, Small JV (1998). Targeting, capture, and stabilization of microtubules at early focal adhesions. J Cell Biol 142, 181–190.
Kirchhofer A, Helma J, Schmidthals K, Frauer C, Cui S, Karcher A, Pellis M, Muyldermans S, Casas-Delucchi CS, Cardoso MC, *et al*. (2010). Modulation of protein properties in living cells using nanobodies. Nat Struct Mol Biol 17, 133–138.
Krylyshkina O, Anderson KI, Kaverina I, Upmann I, Manstein DJ, Small JV, Toomre DK (2003). Nanometer targeting of microtubules to focal adhesions. J Cell Biol 161, 853–859.
Lassing I, Lindberg U (1988). Specificity of the interaction between phosphatidylinositol 4,5-bisphosphate and the profilin:actin complex. J Cell Biochem 37, 255–267.
Le Clainche C, Carlier MF (2008). Regulation of actin assembly associated with protrusion and adhesion in cell migration. Physiol Rev 88, 489–513.
Li Y, Grenklo S, Higgins T, Karlsson R (2008). The profilin:actin complex localizes to sites of dynamic actin polymerization at the leading edge of migrating cells and pathogen-induced actin tails. Eur J Cell Biol 87, 893–904.
Lindberg U, Karlsson R, Lassing I, Schutt CE, Hoglund AS (2008). The microfilament system and malignancy. Semin Cancer Biol 18, 2–11.
Lu J, Pollard TD (2001). Profilin binding to poly-L-proline and actin monomers along with ability to catalyze actin nucleotide exchange is required for viability of fission yeast. Mol Biol Cell 12, 1161–1175.
Markey F, Persson T, Lindberg U (1981). Characterization of platelet extracts before and after stimulation with respect to the possible role of profilactin as microfilament precursor. Cell 23, 145–153.
Martin M, Ahern-Djamali SM, Hoffmann FM, Saxton WM (2005). Abl tyrosine kinase and its substrate Ena/VASP have functional interactions with kinesin-1. Mol Biol Cell 16, 4225–4230.
Mayboroda O, Schluter K, Jockusch BM (1997). Differential colocalization of profilin with microfilaments in PtK2 cells. Cell Motil Cytoskeleton 37, 166–177.
Melki R, Fievez S, Carlier MF (1996). Continuous monitoring of Pi release following nucleotide hydrolysis in actin or tubulin assembly using 2-amino-6-mercapto-7-methylpurine ribonucleoside and purine-nucleoside phosphorylase as an enzyme-linked assay. Biochemistry 35, 12038–12045.
Mikati MA, Breitsprecher D, Jansen S, Reisler E, Goode BL (2015). Coronin enhances actin filament severing by recruiting cofilin to filament sides and altering F-actin conformation. J Mol Biol 427, 3137–3147.
Nyman T, Page R, Schutt CE, Karlsson R, Lindberg U (2002a). A cross-linked profilin-actin heterodimer interferes with elongation at the fast-growing end of F-actin. J Biol Chem 277, 15828–15833.
Nyman T, Schuler H, Korenbaum E, Schutt CE, Karlsson R, Lindberg U (2002b). The role of MeH73 in actin polymerization and ATP hydrolysis. J Mol Biol 317, 577–589.
Okada K, Bartolini F, Deaconescu AM, Moseley JB, Dogic Z, Grigorieff N, Gundersen GG, Goode BL (2010). Adenomatous polyposis coli protein nucleates actin assembly and synergizes with the formin mDia1. J Cell Biol 189, 1087–1096.
Pernier J, Shekhar S, Jegou A, Guichard B, Carlier MF (2016). Profilin interaction with actin filament barbed end controls dynamic instability, capping, branching, and motility. Dev Cell 36, 201–214.
Pollard TD, Borisy GG (2003). Cellular motility driven by assembly and disassembly of actin filaments. Cell 112, 453–465.
Raynaud-Messina B, Mazzolini L, Moisand A, Cirinesi AM, Wright M (2004). Elongation of centriolar microtubule triplets contributes to the formation of the mitotic spindle in gamma-tubulin-depleted cells. J Cell Sci 117, 5497–5507.
Rizvi SA, Neidt EM, Cui J, Feiger Z, Skau CT, Gardel ML, Kozmin SA, Kovar DR (2009). Identification and characterization of a small molecule inhibitor of formin-mediated actin assembly. Chem Biol 16, 1158–1168.
Rodriguez OC, Schaefer AW, Mandato CA, Forscher P, Bement WM, Waterman-Storer CM (2003). Conserved microtubule-actin interactions in cell movement and morphogenesis. Nat Cell Biol 5, 599–609.
Rottner K, Hanisch J, Campellone KG (2010). WASH, WHAMM and JMY: regulation of Arp2/3 complex and beyond. Trends Cell Biol 20, 650–661.
Rotty JD, Wu C, Haynes EM, Suarez C, Winkelman JD, Johnson HE, Haugh JM, Kovar DR, Bear JE (2015). Profilin-1 serves as a gatekeeper for actin assembly by Arp2/3-dependent and -independent pathways. Dev Cell 32, 54–67.
Shekhar S, Pernier J, Carlier MF (2016). Regulators of actin filament barbed ends at a glance. J Cell Sci 129, 1085–1091.
Shen QT, Hsiue PP, Sindelar CV, Welch MD, Campellone KG, Wang HW (2012). Structural insights into WHAMM-mediated cytoskeletal coordination during membrane remodeling. J Cell Biol 199, 111–124.
Skare P, Kreivi JP, Bergstrom A, Karlsson R (2003). Profilin I colocalizes with speckles and Cajal bodies: a possible role in pre-mRNA splicing. Exp Cell Res 286, 12–21.
Small JV, Geiger B, Kaverina I, Bershadsky A (2002). How do microtubules guide migrating cells? Nat Rev Mol Cell Biol 3, 957–964.
Soderberg O, Gullberg M, Jarvius M, Ridderstrale K, Leuchowius KJ, Jarvius J, Wester K, Hydbring P, Bahram F, Larsson LG, *et al*. (2006). Direct observation of individual endogenous protein complexes in situ by proximity ligation. Nat Methods 3, 995–1000.
Suarez C, Carroll RT, Burke TA, Christensen JR, Bestul AJ, Sees JA, James ML, Sirotkin V, Kovar DR (2015). Profilin regulates F-actin network homeostasis by favoring formin over Arp2/3 complex. Dev Cell 32, 43–53.
Suetsugu S, Miki H, Takenawa T (1998). The essential role of profilin in the assembly of actin for microspike formation. EMBO J 17, 6516–6526.
Thurston SF, Kulacz WA, Shaikh S, Lee JM, Copeland JW (2012). The ability to induce microtubule acetylation is a general feature of formin proteins. PLoS One 7, e48041.
Tint IS, Bershadsky AD, Gelfand IM, Vasiliev JM (1991). Post-translational modification of microtubules is a component of synergic alterations of cytoskeleton leading to formation of cytoplasmic processes in fibroblasts. Proc Natl Acad Sci USA 88, 6318–6322.
Vasiliev JM, Gelfand IM, Domnina LV, Ivanova OY, Komm SG, Olshevskaja LV (1970). Effect of colcemid on the locomotory behaviour of fibroblasts. J Embryol Exp Morphol 24, 625–640.
Wen Y, Eng CH, Schmoranzer J, Cabrera-Poch N, Morris EJ, Chen M, Wallar BJ, Alberts AS, Gundersen GG (2004). EB1 and APC bind to mDia to stabilize microtubules downstream of Rho and promote cell migration. Nat Cell Biol 6, 820–830.
Wersinger C, Sidhu A (2005). Disruption of the interaction of alpha-synuclein with microtubules enhances cell surface recruitment of the dopamine transporter. Biochemistry 44, 13612–13624.
Witke W (2004). The role of profilin complexes in cell motility and other cellular processes. Trends Cell Biol 14, 461–469.
Witke W, Podtelejnikov AV, Di Nardo A, Sutherland JD, Gurniak CB, Dotti C, Mann M (1998). In mouse brain profilin I and profilin II associate with regulators of the endocytic pathway and actin assembly. EMBO J 17, 967–976.
Wittenmayer N, Rothkegel M, Jockusch BM, Schluter K (2000). Functional characterization of green fluorescent protein-profilin fusion proteins. Eur J Biochem 267, 5247–5256.
Yarar D, D'Alessio JA, Jeng RL, Welch MD (2002). Motility determinants in WASP family proteins. Mol Biol Cell 13, 4045–4059.